Peremennye Zvezdy (*Variable Stars*) **44**, No. 6, 2024

Received 3 June; accepted 23 September.

DOI: 10.24412/2221-0474-2024-44-56-77

Catalog of Multi–mode Radially Pulsating Variables: II

A. V. Khruslov[1,2]

[1] Sternberg Astronomical Institute, Moscow State University, Universitetskij pr. 13, Moscow 119992, Russia; khruslov@bk.ru

[2] Institute of Astronomy, Russian Academy of Sciences, Pyatnitskaya str. 48, Moscow 119017, Russia

I present the second part of the catalog of newly detected Multi-Mode Radially Pulsating (MMRP) variable stars. For these stars, pulsations in the fundamental, first-, second-, or third-overtone modes were detected. This paper includes 60 double- and multi-mode stars (numbered from MMRP–051 to MMRP–110). Variability types determined for these stars are RR Lyrae variables and high-amplitude δ Scuti (HADS) stars. In addition, one of the previously studied stars, MMRP-010, was reclassified.

I analyzed all observations available for these stars in the ASAS-SN and ZTF online public archives using the period-search software developed by Dr. V.P. Goranskij for Windows environment. Light elements and parameters of oscillations were determined.

1 Introduction

The second part of the catalog of Multi–Mode Radially Pulsating (MMRP) variables is the continuation of my previous paper (Khruslov 2023), the first part of the MMRP catalog, and presents my detection of 60 new double- and multi-mode variables. The star numbers in the second part of the catalog are from MMRP–051 to MMRP–110.

Among these stars, there are RR Lyrae variables and high-amplitude δ Scuti (HADS) variables. These are stars that pulsate in the fundamental mode, the first-, second-, or third-overtone mode.

The method I apply to search for multi-periodicity, the photometric data used, identification names of stars included in the catalog, classification system, and multi-row structure of the tables, with a set of sub-rows, each of them corresponding to a individual detected radial pulsation mode, are the same as those described in the first part of the MMRP catalog.

Searching for double periodicity, I mainly used data available in the photometric archives of the All-Sky Automated Survey for Supernovae (ASAS–SN[1], Shappee et al. 2014; Kochanek et al. 2017) and the Zwicky Transient Facility (ZTF, Bellm et al. 2019; Masci et al. 2019). The ZTF data were taken from the SNAD ZTF viewer[2], Malanchev et al. (2021). The light elements are based on data from these two surveys. The magnitude ranges and amplitudes of brightness variations are given in the tables according to these data. Additionally, in individual cases, I analyzed available data from other archives: the Wide Angle Search for Planets (SuperWASP[3], Butters et al. 2010; 7 variables), the

[1] https://asas-sn.osu.edu/
[2] https://ztf.snad.space/
[3] http://wasp.cerit-sc.cz/form/

Catalina Sky Surveys (CSS[4], Drake et al. 2009; 6 variables). The SuperWASP observations are available as FITS tables, which were converted into ASCII tables using the OMC2ASCII[5] program as described by Sokolovsky (2007).

In some cases, continuous data series from ZTF, with duration of a whole night of observations, were recalculated as average values that were used for subsequent analysis; they are presented in the data files below the main data series.

The survey data used in this study for the program stars are available online in the html version of this paper as a zip archive. The archive also contains light curves of all variables and a cross-identification table for all stars.

2 Format of presentation

2.1 Identification names

The MMRP catalog uses two types of variable-star identification names:

(1) the format for designating stars whose multiperiodicity was first discovered in this study is:

MMRP–XXX

(2) and the format for designating known multiperiodic stars, for which new light elements are presented, is:

MMRP JXXXXXX.XX+XXXXXX.X

(equatorial coordinates for equinox 2000.0).

Designations of the type (2) appeared only in the first part of the MMRP.

2.2 Classification

New original MMRP classification of multiperiodic variables is somewhat more detailed than that used in the General Catalog of Variable Stars, GCVS (Samus et al. 2017), but is based on the principles presented by N.N. Samus and the GCVS team at the XXVI IAU General Assembly in Prague, 2006[6]. The studies that have resulted in the MMRP catalog are a part of the program aimed at inclusion of new variables into the GCVS.

The MMRP classification consists of the variability type designated with a single letter (C – Classical Cepheids; W – W Virginis type II Cepheids; R – RR Lyrae stars; D – δ Scuti stars) and the numerical identification of pulsation modes (0 – fundamental mode; 1 – first overtone; 2 – second overtone; 3 – third overtone). Extra characteristics are introduced with an additional index (n – additional non-radial mode; m – amplitude modulation with a slow variation from season to season). An arrow $\rightarrow$ indicates the cases of mode switching. Examples: C01, C12m, D0123, D01n, R01, R01$\rightarrow$R0.

The radial pulsation modes were identified on the base of the period ratio ($P_{\rm short}/P_{\rm long}$); see the study of this problem in Petersen (1973), Petersen & Christensen-Dalsgaard (1996), Smolec & Moskalik (2010), etc.

[4]http://nunuku.caltech.edu/cgi-bin/getcssconedb_release_img.cgi
[5]http://scan.sai.msu.ru/swasp_converter/
[6]http://www.sai.msu.su/gcvs/future/classif.htm

2.3 Tables

We use a multi-row format in the Tables of the MMRP catalog. For a complete description of the format, see the first part of the MMRP catalog (Khruslov 2023).

The main table (Table 1) contains general information on the star: number in the MMRP Catalog; equatorial coordinates J2000; magnitude range; type of multi-periodicity; and then, information about individual modes is presented in sub-rows (light elements, period and epoch of maximum; semi-amplitude; asymmetry parameter of the phased light curve, M–m). The period ratio P_S/P_L (shorter period / longer period) is given for each pair of adjacent sub-rows (in the sub-row for the longer period).

The equatorial coordinates are given according to the Gaia DR3 catalog. The tabulated magnitude range is for the photometric band indicated in brackets (aV and ag are ASAS–SN V and g magnitudes; zr and zg are ZTF r and g magnitudes). Semi-amplitudes are given in the photometric band indicated in the Magn. column.

In addition to the notation used in the MMRP–I catalog, the second part (this paper) contains epochs in the following three formats:

$E_a = aX.XXXX = \mathrm{HJD} - 2457777.0$;

$E_b = bX.XXXX = \mathrm{HJD} - 2458888.0$;

$E_c = cX.XXXX = \mathrm{HJD} - 2460000.0$.

In the second part of the MMRP, I do not present separate tables of comments in the format of coded numbers (Tables 2 and 2a in MMRP–I). After Table 1, I present comments for individual stars. I excluded information about the history of variability studies for individual stars that was included in the Comments of the first MMRP catalog. This information can be found in the web sources of the photometric surveys: the ASAS–SN catalogs of variable stars[7] (Jayasinghe et al. 2018, 2019a, 2019b, 2020, 2021); the ZTF catalog of periodic variable stars[8], Chen et al. (2020); Gaia DR2 and Gaia DR3, and others. Identifications with these catalogs can be found in the cross-identification table available online in the html version of this paper (see the link in Section 1).

The supplementary Tables 2 and 3 (corresponding respectively to Tables 3 and 4 in MMRP–I) contain semi-amplitudes and magnitude ranges in all bands used in the ASAS–SN and ZTF surveys and known information from catalogs and photometric surveys: color indices and Galactic latitudes.

2.4 Light curves

An example of light curves for one of the stars, MMRP–075, is displayed in Fig. 1. The star is classified as a D13 type variable. The top panels present data folded with the first- and third-overtone periods. The bottom panels show the same curves after prewhitening the other oscillation (also, the $f_3{+}f_1$, $f_3{-}f_1$, $f_3{+}2f_1$, and $2f_1{-}f_3$ interaction frequencies were excluded). Along with the light curves, we present power spectra of the double-mode variables, for the raw data and after subtraction of the dominant mode (the first-overtone oscillation in the case of MMRP–075). The structure of the power spectra shows that the secondary periods are real.

The light curves for all studied stars are available online in the html version of this paper as a zip archive (see the link in Section 1). The light curves are given in the format displayed in Fig. 1. A similar and more complete format is used for triple- and quadruple-mode variables.

[7] https://asas-sn.osu.edu/variables

[8] http://variables.cn:88/ztf/

3 Results

Among the 60 stars presented in this paper, there are 10 RR Lyrae stars of the R01 type, 50 high-amplitude δ Scuti stars (double-mode: 22 stars of the D01 type; 8 D12 stars; 3 D02 stars; 10 D13 stars; triple-mode: one D012 star and 5 D123 stars; one quadruple-mode D0123 star). Stars of the D02 and D13 types have not been studied by me before. Double-mode or multi-mode Cepheids are not presented in this paper.

In addition, one of the previously studied stars, MMRP–010, was reclassified as a D01 star.

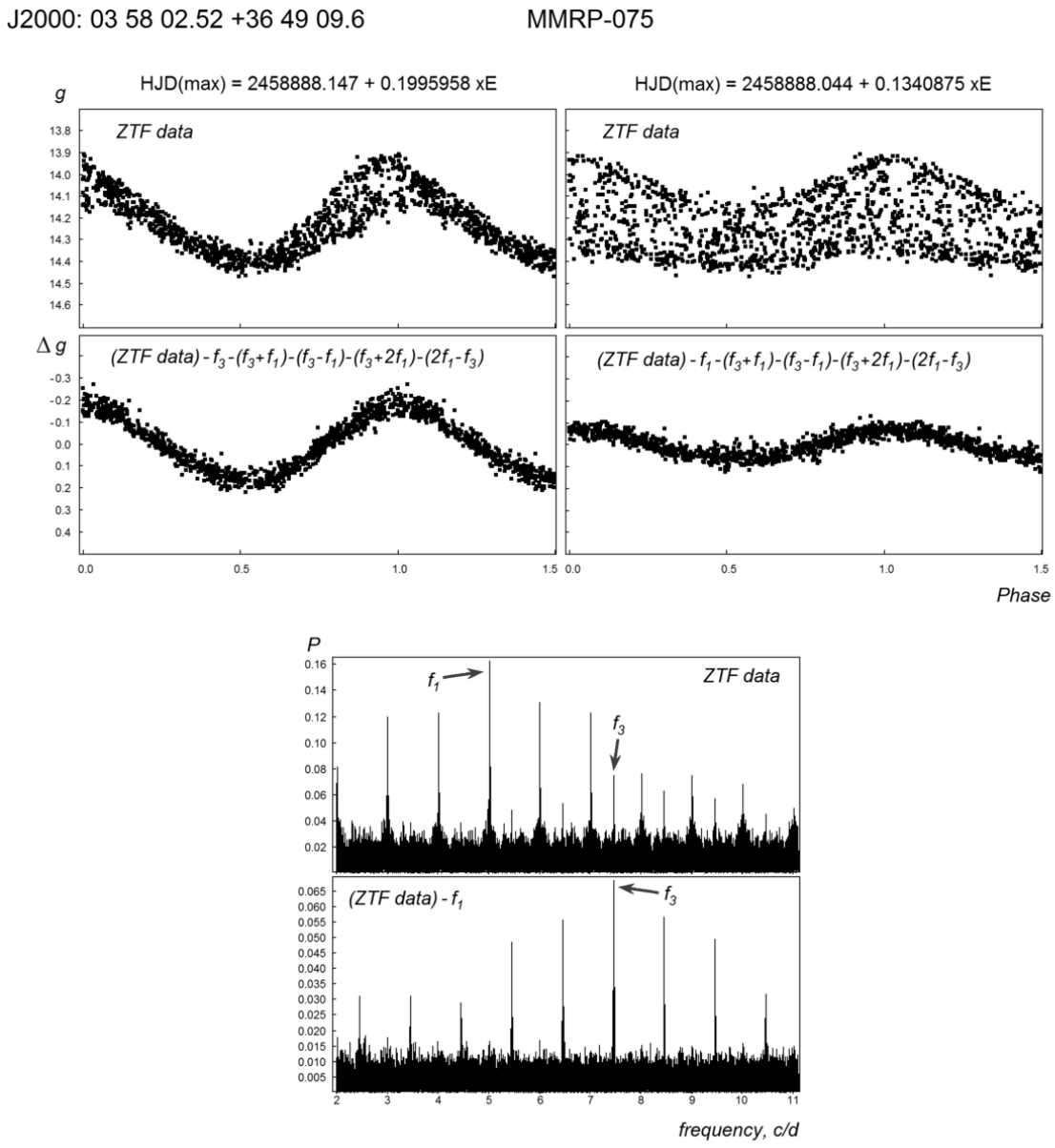

Figure 1. The light curves and power spectra of the star MMRP–075 (D13 type) from g-band ZTF data.

Table 1: **MMRP variables**

No.	J2000	Magn.	Type	Period, d	Epoch	Ampl.	M–m	P_S/P_L
010	04 53 16.75	14.37 –	D01	0.323070	b0.036	0.164	0.37	0.7547
	+39 14 18.2	15.21 (ag)		0.243812	b0.100	0.136	0.55	
051	00 06 39.46	17.67 –	D13	0.0675897	b0.0012	0.210	0.38	0.6749
	+53 13 44.0	18.24 (zg)		0.0456185	b0.0414	0.018	0.50	
052	00 09 33.51	17.84 –	D01	0.0836583	b0.0165	0.139	0.39	0.7749
	+56 21 44.4	18.43 (zg)		0.0648244	b0.0040	0.054	0.44	
053	00 10 52.50	17.63 –	D01	0.1539483	b0.0427	0.140	0.38	0.7688
	+56 31 18.5	18.50 (zg)		0.1183604	b0.0285	0.162	0.35	
054	00 14 24.72	16.05 –	D01	0.0859502	b0.0654	0.183	0.36	0.7742
	+53 20 52.7	16.50 (zg)		0.0665394	b0.0105	0.017	0.50	
055	00 23 45.18	17.33 –	D01	0.1097914	b0.1045	0.060	0.40	0.7735
	+64 45 54.9	17.83 (zg)		0.0849198	b0.0690	0.112	0.40	
056	00 27 07.81	15.47 –	D012	0.1165398	b0.0500	0.035	0.47	0.7703
	+57 37 40.7	15.90 (zg)		0.0897679	b0.0499	0.140	0.39	0.8015
				0.0719476	b0.0645	0.016	0.50	
057	00 29 28.85	17.18 –	D01	0.06204725	b0.0154	0.170	0.38	0.7766
	+54 18 42.6	17.69 (zg)		0.0481865	b0.0170	0.031	0.48	
058	00 29 30.75	15.91 –	R01	0.465953	b0.067	0.132	0.40	0.7434
	+50 45 40.7	16.60 (zr)		0.346377	b0.097	0.159	0.39	
059	00 35 42.60	17.76 –	D01	0.1457098	b0.127	0.053	0.42	0.7709
	+64 27 12.6	18.08 (zr)		0.1123257	b0.043	0.042	0.39	
060	00 37 28.27	17.77 –	D01	0.0766737	b0.0408	0.245	0.34	0.7500
	+55 20 00.3	18.52 (zg)		0.0575075	b0.0340	0.029	0.46	
061	00 45 27.68	16.31 –	D01	0.0946369	b0.0235	0.154	0.37	0.7719
	+58 53 58.9	17.20 (zg)		0.0730509	b0.0304	0.146	0.35	
062	00 48 11.14	13.58 –	D13	0.0793879	b0.0215	0.245	0.37	0.6714
	+47 37 19.0	14.25 (ag)		0.0533018	b0.0097	0.025	0.50:	
063	00 50 42.33	17.79 –	D13	0.0845786	b0.0470	0.175	0.40	0.6514
	+56 51 08.9	18.30 (zg)		0.0550910	b0.0260	0.018	0.50	
064	00 51 37.66	17.35 –	D12	0.0930969	b0.0701	0.211	0.40	0.8035
	+68 45 17.0	17.95 (zg)		0.0748047	b0.0738	0.023	0.43:	

Table 1: **MMRP variables**

No.	J2000	Magn.	Type	Period, d	Epoch	Ampl.	M–m	P_S/P_L
065	00 51 41.52	16.88 –	D01	0.0853045	b0.0130	0.174	0.36	0.7744
	+52 43 16.3	17.55 (zg)		0.0660640	b0.0406	0.082	0.41	
066	01 00 46.09	18.13 –	D01	0.0653560	b0.0567	0.120	0.37	0.7525
	+71 59 36.6	18.54 (zr)		0.0491802	b0.0315	0.016	0.44	
067	02 37 13.67	15.38 –	D12	0.0985287	b0.0244	0.140	0.38	0.8035
	+63 02 49.9	15.75 (zr)		0.0791710	b0.0138	0.010	0.50	
068	02 43 26.13	18.00 –	D12	0.0821909	b0.0283	0.214	0.35	0.8027
	+65 21 01.1	18.63 (zr)		0.0659757	b0.0205	0.015	0.50	
069	02 46 59.99	17.34 –	D13m	0.0841481	b0.0759	0.221	0.38	0.6736
	+61 35 38.7	17.95 (zg)		0.0566862	b0.0105	0.042	0.48	
070	03 20 12.89	16.62 –	D13	0.0662601	b0.0240	0.070	0.43	0.6581
	+62 34 13.0	16.84 (zr)		0.0436084	b0.0097	0.015	0.47	
071	03 23 43.84	18.10 –	D01	0.1094991	b0.0757	0.059	0.47	0.7730
	+62 52 47.9	18.45 (zr)		0.0846419	b0.0545	0.053	0.48	
072	03 34 42.83	17.43 –	D01	0.1028625	b0.0866	0.099	0.39	0.7715
	+60 31 08.3	17.77 (zr)		0.0793606	b0.0250	0.026	0.46	
073	03 43 18.44	16.34 –	D13	0.0911844	b0.0530	0.065	0.45	0.6484
	+68 31 57.1	16.56 (zr)		0.0591228	b0.0183	0.019	0.47	
074	03 52 55.98	18.09 –	D01	0.1074287	b0.0740	0.152	0.35	0.7730
	+55 03 33.5	18.63 (zr)		0.0830433	b0.0470	0.054	0.39	
075	03 58 02.52	13.92 –	D13	0.1995958	b0.147	0.168	0.48	0.6718
	+36 49 09.6	14.45 (zg)		0.1340875	b0.044	0.061	0.45	
076	04 05 46.65	16.45 –	D12	0.1301875	b0.0945	0.167	0.43	0.8038
	+57 40 21.6	16.90 (zg)		0.104641	b0.0592	0.023	0.46	
077	04 09 46.34	17.02 –	D12	0.0740534	b0.0345	0.119	0.37	0.8073
	+53 07 47.6	17.37 (zr)		0.0597822	b0.0587	0.012	0.44	
078	04 18 00.38	16.27 –	D0123	0.1224802	b0.0825	0.051	0.42	0.7722
	+56 08 42.3	16.60 (zr)		0.0945762	b0.0225	0.057	0.42	0.8048
				0.0761115	b0.0693	0.023	0.47	0.8336
				0.0634467	b0.0250	0.029	0.50	
079	04 19 16.52	17.41 –	D01	0.0838792	b0.0404	0.137	0.31	0.7747
	+57 14 23.1	17.83 (zr)		0.0649833	b0.0145	0.018	0.48	

Table 1: **MMRP variables**

No.	J2000	Magn.	Type	Period, d	Epoch	Ampl.	M–m	P_S/P_L
080	05 15 27.80	16.59 –	D01	0.0701374	b0.0374	0.234	0.32	0.7763
	+70 36 58.8	17.42 (zg)		0.0544502	b0.0325	0.058	0.46	
081	05 28 53.05	13.20 –	D123	0.1482472	b0.144	0.076	0.43	0.8018
	+48 36 11.8	13.41 (zr)		0.1188605	b0.105	0.009	0.50	0.8322
				0.0989185	b0.019	0.013	0.48	
082	07 14 14.39	13.72 –	D12m	0.0915925	b0.0885	0.224	0.35	0.8055
	+73 27 29.6	14.33 (zg)		0.0737798	b0.0296	0.035	0.50	
083	09 48 09.85	13.36 –	D13n	0.08640150	b0.0125	0.101	0.44	0.6601
	–61 19 30.3	13.69 (ag)		0.05703713	b0.0540	0.011	0.53:	
084	14 01 22.52	18.60 –	R01	0.542780	b0.245	0.058	0.50:	0.7467
	+26 39 00.5	19.40 (zg)		0.405293	b0.212	0.224	0.39	
085	14 03 54.78	16.74 –	R01	0.489193	b0.160	0.194	0.41	0.7437
	+67 08 42.6	17.73 (zg)		0.363813	b0.072	0.235	0.39	
086	14 31 33.52	12.80 –	D02n:	0.09348775	b0.0181	0.135	0.41	0.6102
	–44 14 40.3	13.18 (ag)		0.05704222	b0.0082	0.013	0.48	
087	14 50 44.40	14.29 –	D02	0.1817898	b0.071	0.235	0.32	0.5987
	–51 09 56.0	15.01 (ag)		0.1088370	b0.044	0.025	0.43	
088	15 03 57.99	19.32 –	R01	0.58066	b0.398	0.057	0.40	0.7462
	+67 12 16.7	20.15 (zg)		0.43331	b0.187	0.216	0.35	
089	15 19 31.77	13.61 –	D123	0.1691712	b0.068	0.102	0.47	0.7994
	–62 58 21.0	14.10 (ag)		0.1352296	b0.055	0.037	0.49	0.8316
				0.1124590	b0.073	0.040	0.46	
090	15 46 05.81	16.99 –	R01	0.473777	b0.362	0.182	0.41	0.7440
	+79 22 24.7	18.01 (zg)		0.352505	b0.016	0.220	0.37	
091	15 56 32.39	13.90 –	D01m	0.0707824	a0.0124	0.141	0.38	0.7702
	–38 48 02.0	14.55 (aV)		0.0545141	a0.0330	0.071	0.50:	
092	16 07 49.75	17.29 –	R01	0.486850	b0.070	0.033	0.47	0.7445
	+20 16 56.9	17.89 (zg)		0.362469	b0.170	0.231	0.40	
093	16 26 25.26	16.86 –	R01	0.481098	b0.183	0.151	0.40	0.7444
	+69 44 18.3	17.80 (ag)		0.358113	b0.007	0.222	0.38	
094	16 29 16.93	13.14 –	D02	0.16514947	b0.0733	0.177	0.34	0.6089
	–20 49 49.2	13.61 (ag)		0.1005594	b0.0828	0.020	0.48	

Table 1: **MMRP variables**

No.	J2000	Magn.	Type	Period, d	Epoch	Ampl.	M–m	P_S/P_L
095	16 49 42.63	17.11 –	R01	0.475254	b0.060	0.169	0.40	0.7444
	+47 53 42.6	18.11 (zg)		0.353766	b0.324	0.226	0.38	
096	17 50 31.00	11.76 –	D13	0.1239932	b0.1177	0.075	0.46	0.6593
	–28 11 35.6	12.00 (ag)		0.0817480	b0.0522	0.015	0.45	
097	18 00 55.06	14.48 –	D01	0.1176389	b0.021	0.235	0.36	0.7717
	–56 45 32.7	15.40 (ag)		0.0907838	b0.063	0.063	0.43	
098	18 01 23.93	18.70 –	R01	0.547167	b0.435	0.097	0.43	0.7460
	+46 12 26.2	19.62 (zg)		0.408183	b0.153	0.234	0.37	
099	18 13 15.97	14.47 –	D123	0.1163633	b0.0233	0.060	0.50	0.7996
	–16 04 22.1	14.72 (zr)		0.0930402	b0.0685	0.023	0.49	0.8297
				0.0771944	b0.0418	0.020	0.43	
100	18 32 35.84	12.38 –	D123n	0.1763344	b0.081	0.099	0.46	0.7980
	+23 45 13.1	12.83 (ag)		0.1407097	b0.065	0.028	0.49	0.8225
				0.1157337	b0.020	0.043	0.49	
101	18 41 51.71	19.2 –	R01	0.513113	b0.135	0.045	0.47	0.7458
	+19 34 59.4	19.7 (zr)		0.382661	b0.382	0.143	0.43	
102	18 57 09.54	15.10 –	D01	0.08030705	b0.0360	0.065	0.44	0.7755
	–29 32 13.2	15.60 (ag)		0.06228179	b0.0437	0.062	0.43	
103	19 11 49.38	13.60 –	D01	0.07061797	b0.0125	0.152	0.38	0.7738
	–27 44 44.1	14.16 (ag)		0.05464646	b0.0336	0.051	0.45	
104	19 45 52.97	17.58 –	D01n	0.0815354	b0.0316	0.108	0.41	0.7849
	+16 41 58.7	18.25 (zg)		0.0640002	b0.0307	0.110	0.37	
105	19 45 53.19	14.41 –	D123	0.1565323	b0.0925	0.174	0.39	0.7969
	+19 17 04.3	14.87 (zg)		0.1247345	b0.0870	0.018	0.50:	0.8332
				0.1039327	b0.0077	0.010	0.44:	
106	19 48 42.16	15.67 –	D12	0.1284792	b0.0088	0.128	0.44	0.7982
	+18 20 51.4	16.03 (zg)		0.1025547	b0.0339	0.013	0.45	
107	19 56 54.19	13.92 –	D13n	0.07672450	b0.0440	0.093	0.45	0.6715
	–22 53 31.5	14.24 (ag)		0.05151785	b0.0498	0.019	0.50	
108	20 36 21.97	15.15 –	D01	0.0644808	b0.0219	0.110	0.47	0.7792
	–50 02 15.3	15.80 (ag)		0.0502418	b0.0085	0.115	0.44	
109	23 46 17.96	17.54 –	D01m	0.0911045	b0.0065	0.104	0.44	0.7772

Table 1: **MMRP variables**

No.	J2000	Magn.	Type	Period, d	Epoch	Ampl.	M–m	P_S/P_L
	+53 34 08.9	18.12 (zg)		0.0708039	b0.0327	0.091	0.43	
110	23 46 29.54	16.84 –	D12	0.0892052	b0.0878	0.259	0.38	0.8034
	+64 10 27.3	17.52 (zg)		0.0716654	b0.0567	0.024	0.48	

Comments to Table 1.

MMRP–054. A blend in the ASAS–SN data is possible, amplitude underestimated. Due to large errors, this data is not included in the table.

MMRP–062. The third-overtone period P_3 varies. The elements in the Table are given for the g ASAS–SN and r and g ZTF data time interval. The elements for the V-band ASAS–SN time interval are:

HJD(max) = 2457777.0115 + $0^d.0533036 \times E$.

The first-overtone period P_1 also possibly varies.

MMRP–064. Amplitude modulation with slow variation from one season to another is possible for the second-overtone oscillation f_2. Type D12m is not excluded.

MMRP–067. A blend in the ASAS–SN data is possible, amplitude underestimated.

MMRP–069. The period P_3 varies. Elements for P_1 are given for the whole time interval covered with observations. The Table gives light elements for the first time interval in ZTF data, JD 2458287–2459150. The light elements for the second time interval in ZTF data, JD 2459150–2459995, are:

f_1: HJD(max) = 2459600.0530 + $0^d.0841481 \times E$;

f_3: HJD(max) = 2459600.0160 + $0^d.0566891 \times E$;

$A_1 = 0.155$ and $A_3 = 0.014$ in the zr band, $A_1 = 0.219$ and $A_3 = 0.021$ in the zg band.

MMRP–075. Data from 1SWASP and CSS were used to improve the light elements. Magnitude range and semi-amplitude according to 1SWASP data: $14^m.32$–$15^m.34$ (1SWASP mag); $A_1 = 0.234$, $A_3 = 0.097$. According to CSS data: $13^m.15$–$13^m.56$ (CV); $A_1 = 0.123$, $A_3 = 0.046$. In the 1SWASP data, the oscillation amplitude is the largest.

MMRP–076. A blend in ASAS–SN data is possible, amplitude underestimated.

MMRP–078. Other period ratios: $P_2/P_0 = 0.6214$, $P_3/P_1 = 0.6709$.

MMRP–081. The first overtone period P_1 possibly varies. In the ASAS–SN V-band data (earlier time interval), the second-overtone oscillation f_2 is not detected, amplitude of the third-overtone mode A_3 is the largest. Amplitude modulation is not excluded.

MMRP–082. Amplitude modulation of the second overtone oscillation. The photometry was studied in three time intervals:

I. JD 2455970–2458452. Only aV data. The first overtone elements are:

f_1: HJD(max) = 2457777.0710 + $0^d.0915920 \times E$; M–m = 0.35.
The semi-amplitude is A_1 = 0.190 (aV).

The detection of the second-overtone mode f_2 is very uncertain, the possible period P_2 = $0^d.737833$, $A_2 \leq 0.010$.

II. JD 2458034–2458994. The analysis made use of the ag, zr, and zg data. The light elements and amplitudes for this time interval are presented in the Tables.

III. JD 2459076–2460373. The light elements are the following:

f_1: HJD(max) = 2460000.0290 + $0^d.0915930 \times E$; M–m = 0.37;
The semi-amplitudes are: A_1 = 0.209 (ag), 0.160 (zr), 0.240 (zg).

f_2: HJD(max) = 2460000.0360 + $0^d.07378 \times E$; M–m = 0.50:.
The semi-amplitudes are: $A_2 < 0.008$ (ag), 0.006 (zr), 0.007 (zg).

MMRP–083. There is an additional non-radial pulsation f_n with the following light elements:

HJD(max) = 2458888.0432 + $0^d.05668265 \times E$;
The semi-amplitudes A_n are 0.009 (aV), 0.008 (ag). M–m = 0.49.

MMRP–085. Amplitudes and magnitude range in the i-band of ZTF data: A_0 = 0.102, A_1 = 0.113; $16^m.89$–$17^m.44$.

MMRP–086. Data from 1SWASP were used to improve the light elements. Magnitude range and semi-amplitudes according to 1SWASP data: A_0 = 0.078, A_2 = 0.013; $12^m.59$–$12^m.85$ (1SWASP mag).

An additional, possibly non-radial, pulsation f_n was found with certainty in the g-band ASAS–SN data; in the V-band ASAS–SN and 1SWASP data, it is uncertain. Its light elements are the following:

HJD(max) = 2458888.0410 + $0^d.07345498 \times E$.
The semi-amplitudes A_n are 0.007: (aV), 0.008 (ag), 0.003: (1SWASP mag). The period ratio P_n/P_0 = 0.7857 possibly corresponds to the P_1/P_0 ratio, but P_2/P_n = 0.7766 does not correspond to the P_2/P_1 ratio.

MMRP–088. The amplitudes and magnitude range in the i band of ZTF data: A_0 = 0.039, A_1 = 0.108; $19^m.26$–$19^m.83$.

MMRP–090. The amplitude and magnitude range in the i band of ZTF data: A_0 = 0.085, A_1 = 0.111; $17^m.12$–$17^m.71$.

MMRP–091. Type D01→D0 is not excluded. ASAS–SN data were analyzed in four separate time intervals:

I, JD 2457400–2458100, V band;
II, JD 2458100–2458800, V and g bands;
III, JD 2458800–2459500, g band;
IV, JD 2459600–2460400, g band.

In the data for time interval I, double periodicity was detected, the light elements are given in the Table. In the data for time interval II, the first-overtone oscillation in the g-band data was possibly detected (very uncertainly) with a small amplitude and a different period. The possible period $P_1 = 0^d.0545112$:, A_1 = 0.014 (ag). In V-band data for the time interval II, f_1 was not detected. In the data for the time intervals III and IV, f_1 was not detected.

The fundamental-mode period P_0 varies, the following light elements were derived for separate time intervals:

II: HJD(max) = 2458500.0423 + $0^{\rm d}.0707801 \times E$; $A_0 = 0.201$ (ag), 0.167 (aV);

III: HJD(max) = 2459200.0544 + $0^{\rm d}.0707797 \times E$; $A_0 = 0.201$ (ag);

IV: HJD(max) = 2460000.0212 + $0^{\rm d}.0707817 \times E$; $A_0 = 0.199$ (ag).

In the earlier time interval of 1SWASP data, JD 2453860–2454275, double-mode periodicity was detected with the following elements:

f_0: HJD(max) = 2454054.0025 + $0^{\rm d}.0707800 \times E$; M–m = 0.40,

f_1: HJD(max) = 2454054.0025 + $0^{\rm d}.0545125 \times E$; M–m = 0.45.

The semi-amplitudes are $A_0 = 0.186$, $A_1 = 0.055$ (1SWASP mag).

In the 1SWASP data, after removing the radial frequencies f_0 and f_1 as well as interaction frequencies ($f_1 + f_0$ and $f_1 - f_0$), a possible non-radial oscillation f_n with the period $P_n = 0^{\rm d}.0369620$ is detected, $A_n = 0.018$ (1SWASP mag). In the V-band ASAS–SN data for all time intervals (I and II), this frequency is not detected. In the g-band ASAS–SN data for all time intervals (II, III and IV), this oscillation is detected:

II: $P_n = 0^{\rm d}.0369614$:, $A_n = 0.015$;

III: $P_n = 0^{\rm d}.03696196$, $A_n = 0.020$;

IV: $P_n = 0^{\rm d}.0369631$, $A_n = 0.012$.

MMRP–092. The magnitude range according to CSS data: $17^{\rm m}.06$–$17^{\rm m}.61$ (CV). In CSS data, P_0 is not detected.

MMRP–093. The amplitudes and magnitude range in the i band of ZTF data: $A_0 = 0.081$, $A_1 = 0.115$; $17^{\rm m}.04$–$17^{\rm m}.52$.

MMRP–094. Data from 1SWASP were used to improve the light elements. The amplitudes and magnitude range in the 1SWASP data: $A_0 = 0.146$, $A_2 = 0.016$; $13^{\rm m}.08$–$13^{\rm m}.54$ (1SWASP mag).

MMRP–095. The amplitudes and magnitude range in the i band of ZTF data: $A_0 = 0.091$, $A_1 = 0.119$; $17^{\rm m}.31$–$17^{\rm m}.82$. The amplitudes and magnitude range according to CSS data: $A_0 = 0.099$, $A_1 = 0.137$; $17^{\rm m}.04$–$17^{\rm m}.93$ (CV). Data from CSS were used to improve the light elements.

MMRP–098. The amplitudes and magnitude range in the i band of ZTF data: $A_0 = 0.054$, $A_1 = 0.130$; $18^{\rm m}.79$–$19^{\rm m}.34$. In CSS data, the fundamental mode period P_0 is not detected, magnitude range $18^{\rm m}.7$–$19^{\rm m}.6$ (CV).

MMRP–099. In ASAS–SN V-band data, the second-overtone frequency f_2 is not detected. Amplitude modulation is not excluded.

MMRP–100. An additional non-radial pulsation with the period $P_n = 0^{\rm d}.1351951$, or Blazhko effect of the second-overtone oscillation with $\Pi = 3^{\rm d}.4496$. Semi-amplitude A_n is 0.022 (aV), 0.023 (ag).

Data from 1SWASP were used to improve the light elements. The semi-amplitudes are $A_1 = 0.059$, $A_2 = 0.016$, $A_3 = 0.028$, $A_n = 0.014$. Blend in 1SWASP data.

MMRP–103. According to 1SWASP data, the light elements are:

f_0: HJD(max) = 2454150.0410 + $0^{\rm d}.0706180 \times E$;

f_1: HJD(max) = 2454150.0124 + $0^{\rm d}.0546466 \times E$.

The magnitude range and semi-amplitudes according to 1SWASP data: $13^{\rm m}.75$–$14^{\rm m}.15$, $A_0 = 0.101$, $A_1 = 0.026$.

MMRP–104. A possible non-radial oscillation with the period $P_n = 0^{\rm d}.0520505$; the semi-amplitude A_n is 0.021 (zg), 0.016 (zr). $P_n/P_1 = 0.8133$, identification with the second overtone is not excluded.

MMRP–105. A blend in ASAS–SN data, amplitude underestimated.

MMRP–106. A blend in ASAS–SN data, amplitude underestimated. In the data for zg, zr, and ag bands, the brightening trend was excluded before the amplitude analysis, its full amplitude being 0.018 (zg), 0.021 (zr), and 0.110 (ag). In the aV-band data (an earlier time interval), the trend was not detected.

MMRP–107. An additional non-radial pulsation f_n with the following light elements (ASAS–SN and ZTF data):

HJD(max) = 2458888.032 + $0^{\rm d}.05108950 \times E$;

the semi-amplitude A_n is 0.012 (aV), 0.012 (ag), 0.007 (zr), 0.010 (zg); M–$m = 0.45$.

Light elements for the CSS (JD 2453568–2456446) and 1SWASP (JD 2453860–2454615) time intervals:

f_1: HJD(max) = 2455055.0333 + $0^{\rm d}.0767249 \times E$;

f_3: HJD(max) = 2455055.0225 + $0^{\rm d}.0515180 \times E$;

f_n: HJD(max) = 2455055.0406 + $0^{\rm d}.0510897 \times E$.

The magnitude ranges and semi-amplitudes according to 1SWASP and CSS data: $13^{\rm m}.52$–$13^{\rm m}.82$ (CV), $13^{\rm m}.85$–$14^{\rm m}.18$ (1SWASP mag); A_1 is 0.068 (CV), 0.058 (1SWASP mag); A_3 is 0.018 (CV), 0.015 (1SWASP mag); A_n is 0.013 (CV), 0.007 (1SWASP mag).

MMRP–108. The first-overtone period P_1 possibly varies. Light elements for the CSS time interval:

f_0: JD(max) = 2455055.0276 + $0^{\rm d}.0644806 \times E$;

f_1: JD(max) = 2455055.0075 + $0^{\rm d}.0502488 \times E$.

The magnitude range and semi-amplitudes: $15^{\rm m}.18$–$15^{\rm m}.61$ (CV), $A_0 = 0.072$, $A_1 = 0.070$.

MMRP–109. The amplitude of the first-overtone oscillation varies from season to season, the mean estimates of the amplitude are given in the Table.

MMRP–110. A blend in ASAS–SN data, results of this analysis are not given in the Tables. In these data, the second-overtone frequency f_2 is not detected (as a result of possible large errors of observations).

4 Discussion

4.1 Re–classification of MMRP–010

In the first part of the MMRP catalog (Khruslov 2023), I made a wrong classification of MMRP–010 as a quadruple-mode D0123-type variable. For this star, the frequencies of the supposed radial modes are equidistant, $f_1 - f_0 = f_2 - f_1 = f_3 - f_2 = 1.0062$. Frequencies

f_0 and f_1 are not in doubt, but the frequencies f_2 and f_3 of this equidistant quadruplet can be considered interaction frequencies of the two main oscillations: $f_2 = 2f_1 - f_0$ and $f_3 = 3f_1 - 2f_0$.

Thus, in this case, we have two main frequencies f_0 and f_1; in addition to them, interaction frequencies $f_1 + f_0$, $2f_1 - f_0$, $f_1 - f_0$, $3f_1 - 2f_0$ and $f_1 + 2f_0$ are also detected (in the order of decreasing amplitude).

Usually, the frequencies $2f_1 - f_0$ and especially $3f_1 - 2f_0$ have very small amplitudes and are very rarely detected in data analysis. It is possible that the oscillations in these interaction frequencies are amplified when they coincide with the expected frequencies of the second and third overtones.

For this reason, we re-classified MMRP–010 as a D01-type star. The real D0123 quadruplets (see 14 Galactic-bulge cases in Netzel et al. 2022) are not equidistant. In this paper, I also present a new real case of a D0123 type star, MMRP–078.

Among other features of MMRP–010, the inverted asymmetry (M–m = 0.55) of its first-overtone light curve is worth noting.

4.2 Pulsation modes of MMRP–086

MMRP–086 was classified as a δ Scuti star pulsating in the fundamental and second overtone modes with an additional non-radial pulsation (D02n type). In this case, the additional non-radial pulsation f_n was found with certainty in the g-band ASAS–SN data, but it is not detected or uncertain in the other photometric data (V-band ASAS–SN and 1SWASP). The period ratio $P_n/P_0 = 0.7857$ may correspond to the P_1/P_0 ratio, but $P_2/P_n = 0.7766$ does not correspond to the P_2/P_1 ratio. Therefore, I do not consider f_n as a pulsation in the first overtone and do not classify the star as D012 type. The light curves and power spectra of the star MMRP–086 are displayed in Fig. 2.

4.3 Variables with amplitude modulation

For 4 variables, amplitude modulation with slow changes (from one season to another) was detected. The variability type of these stars contains the index “m”. Among these variables, there are two D01m stars (MMRP–091 and MMRP–109), one D12m star (MMRP–082 = V611 Cam), and one D13m star (MMRP–069).

In some cases, a periodic amplitude variation is possible; however, also in a number of cases, it can represent mode switching. For example, in the case of MMRP–091, during the last time interval, the first-overtone oscillation was not detected, mode switching is possible, type D01→D0 is not excluded. Follow-up monitoring of the object is necessary.

4.4 The Petersen diagram

The Petersen diagram for all detected MMRP variables is displayed in Fig. 3. The diagram shows sequences corresponding to individual types of multi-periodic radially pulsating variables.

4.5 A note to this paper

When this paper was already submitted to Peremennye Zvezdy, Jia et al. (2024) published a catalogue of multimode δ Sct stars from the Zwicky Transient Facility Survey. A number

of stars from our publication were included in this work. These are objects MMRP 051–057, 059, 060, 062, 064, 066, 067, 070, 071, 074, 076–079, 082, 104, 105, and 110. In most cases, the results (classification of pulsation modes and light elements) are almost identical. However, MMRP-104 was classified by Jia et al. (2024) as a triple-mode pulsating star that varied in the fundamental, first- and second-overtone modes, while I identified the third pulsation as a non-radial mode (because of the period ratio $P_3/P_2 = 0.8133$) and gave the star the D01n type; MMRP–105 was classified by Jia et al. (2024) as a double-mode δ Scuti star pulsating in the first and second overtones, while I give the type D123 (the third-overtone mode is real, see power spectra in the zg and zr bands). Also, the cited authors did not detect the amplitude modulation of MMRP–082.

Additionally, for seven of these stars (MMRP–054, 056, 062, 067, 076, 082, and 105), I used data from ASAS-SN to improve their light elements.

Acknowledgments: The author wishes to thank Dr. V.P. Goranskij for providing his software.

References:

Bellm, E. C., Kulkarni, S. R., & Graham, M. J. 2019, *Publ. Astron. Soc. Pacific*, **131**, 018002

Butters, O. W., West, R. G., Anderson, D. R., et al. 2010, *Astron. & Astrophys.*, **520**, L10

Chen, X., Wang, S., Deng, L., et al. 2020, *Astrophys. J., Suppl. Ser.*, **249**, id. 18

Drake, A. J., Djorgovski, S. G., Mahabal, A., et al. 2009, *Astrophys. J.*, **696**, 870

Gaia Collaboration, Brown, A.G.A., Vallenari, A., Prusti, T., et al. 2018, *Astron. & Astrophys.*, **616**, id. A1

Gaia Collaboration, 2022, Gaia DR3 Part 4. Variability, VizieR On-line Data Catalog: I/358

Jayasinghe, T., Kochanek, C. S., Stanek, K. Z., et al. 2018, *Mon. Notices Roy. Astron. Soc.*, **477**, 3145

Jayasinghe, T., Kochanek, C. S., Stanek, K. Z., et al. 2021, *Mon. Notices Roy. Astron. Soc.*, **503**, 200

Jayasinghe, T., Stanek, K. Z., & Kochanek, C. S. 2019a, *Mon. Notices Roy. Astron. Soc.*, **486**, 1907

Jayasinghe, T., Stanek, K. Z., & Kochanek, C. S. 2019b, *Mon. Notices Roy. Astron. Soc.*, **485**, 961

Jayasinghe, T., Stanek, K. Z., & Kochanek, C. S. 2020, *Mon. Notices Roy. Astron. Soc.*, **491**, 13

Jia, Q., Chen, X., Wang, S., et al. 2024, *Astrophys. J., Suppl. Ser.*, **273**, id. 7

Khruslov, A. V. 2023, *Perem. Zvezdy*, **43**, No. 7, 55

Kochanek, C. S., Shappee, B. J., Stanek, K. Z., et al. 2017, *Publ. Astron. Soc. Pacific*, **129**, 104502

Malanchev, K. L., Pruzhinskaya, M. V., Korolev, V. S., et al. 2021, *Mon. Notices Roy. Astron. Soc.*, **502**, 5147

Masci, F. J., Laher, R. R., & Rusholme, B. 2019, *Publ. Astron. Soc. Pacific*, **131**, 018003

Netzel, H., Pietrukowicz, P., Soszyński, I., & Wrona, M. 2022, Monthly Notices Roy. Astron. Soc., 510, 1748

Petersen, J. O. 1973, *Astron. & Astrophys.*, **27**, 89

Petersen, J. O., & Christensen-Dalsgaard, J. 1996, *Astron. & Astrophys.*, **312**, 463

Samus, N. N., Kazarovets, E. V., Durlevich, O. V., Kireeva, N. N., Pastukhova, E. N. 2017, *Astron. Rep.*, **61**, 80
Shappee, B. J., Prieto, J. L., Grupe, D., et al. 2014, *Astrophys. J.*, **788**, 48
Smolec, R. & Moskalik, P. 2010, *Astron. & Astrophys.*, **524**, A40
Sokolovsky, K. V., 2007, *Perem. Zvezdy Prilozh.*, **7**, No. 30

4.6 Supplement Tables

Table 2: **Semi-amplitudes and magnitude ranges**

No.	Semi-amplitudes				Magnitude ranges			
	aV	ag	zr	zg	aV	ag	zr	zg
010	0.143	0.164	0.112	0.162	14.00–	14.37–	13.68–	14.32–
	0.120	0.136	0.102	0.130	14.74	15.21	14.26	15.17
051	–	–	0.142	0.210	–	–	17.32–	17.67–
	–	–	0.012	0.018			17.71	18.24
052	–	–	0.089	0.139	–	–	17.51–	17.84–
	–	–	0.035	0.054			17.89	18.43
053	–	–	0.095	0.140	–	–	17.12–	17.63–
	–	–	0.117	0.162			17.72	18.50
054	–	–	0.121	0.183	–	–	15.85–	16.05–
	–	–	0.009	0.017			16.15	16.50
055	–	–	0.043	0.060	–	–	16.23–	17.33–
	–	–	0.079	0.112			16.56	17.83
056	0.033	0.045	0.023	0.035	15.18–	15.44–	14.99–	15.47–
	0.115	0.131	0.087	0.140	15.72	16.00	15.32	15.90
	$\leq$0.016	0.014:	0.012	0.016				
057	–	–	0.115	0.170	–	–	16.97–	17.18–
	–	–	0.023	0.031			17.31	17.69
058	–	–	0.132	0.179	–	–	15.91–	16.02–
	–	–	0.159	0.222			16.60	16.97
059	–	–	0.053	0.080	–	–	17.76–	19.27–
	–	–	0.042	0.063			18.08	19.73
060	–	–	0.181	0.245	–	–	17.19–	17.77–
	–	–	0.017	0.029			17.73	18.52
061	–	0.118	0.103	0.154	16.2:–	16.4–	15.92–	16.31–
	–	0.118	0.103	0.146	16.7:	17.2	16.55	17.20
062	0.225	0.245	0.173	0.239	13.47–	13.58–	13.58–	13.55–
	0.015	0.025	0.018	0.031	14.06	14.25	14.03	14.20
063	–	–	0.118	0.175	–	–	15.26–	17.79–
	–	–	0.009	0.018			15.63	18.30
064	–	–	0.142	0.211	–	–	16.45–	17.35–
	–	–	0.016	0.023			16.83	17.95
065	–	–	0.116	0.174	–	–	16.63–	16.88–
	–	–	0.053	0.082			17.12	17.55
066	–	–	0.120	0.162	–	–	18.13–	18.44–
	–	–	0.016	0.016:			18.54	18.98
067	0.113	0.168	0.140	0.204	15.6–	16.0–	15.38–	16.03–
	$<$0.040	$\leq$0.020	0.010	0.011	15.9	16.4	15.75	16.57
068	–	–	0.214	0.308	–	–	18.00–	19.3–
	–	–	0.015	0.019:			18.63	20.2
069	–	–	0.153	0.221	–	–	16.52–	17.34–
	–	–	0.024	0.042			16.96	17.95
070	–	–	0.070	0.105	–	–	16.62–	17.59–
	–	–	0.015	0.018			16.84	17.93
071	–	–	0.059	0.086	–	–	18.10–	19.27–

Table 2: **Semi-amplitudes and magnitude ranges**

No.	Semi-amplitudes				Magnitude ranges			
	aV	ag	zr	zg	aV	ag	zr	zg
	–	–	0.053	0.070			18.45	19.85
072	–	–	0.099	0.145	–	–	17.43–	18.32–
	–	–	0.026	0.042			17.77	18.85
073	–	–	0.065	0.093	–	–	16.34–	16.94–
	–	–	0.019	0.028			16.56	17.24
074	–	–	0.152	0.248	–	–	18.09–	19.83–
	–	–	0.054	0.101			18.63	20.85
075	0.150	0.170	0.101	0.168	13.69–	14.00–	13.56–	13.92–
	0.044	0.063	0.042	0.061	14.20	14.59	13.93	14.45
076	0.097:	0.109:	0.120	0.167	15.65–	16.0–	15.64–	16.45–
	0.018:	0.017:	0.017	0.023	16.05:	16.5	15.97	16.90
077	–	–	0.119	0.176	–	–	17.02–	17.86–
	–	–	0.012	0.016			17.37	18.38
078	–	–	0.051	0.068	–	–	16.27–	17.11–
	–	–	0.057	0.083			16.60	17.56
	–	–	0.023	0.033				
	–	–	0.029	0.042				
079	–	–	0.137	0.200	–	–	17.41–	18.09–
	–	–	0.018	0.021			17.83	18.70
080	–	–	0.177	0.234	–	–	16.60–	16.59–
	–	–	0.042	0.058			17.17	17.42
081	0.090	0.101	0.076	0.106	13.28–	13.55–	13.20–	13.64–
	$\leq$0.007	0.012	0.009	0.010	13.56	13.91	13.41	13.97
	0.021	0.018	0.013	0.018				
082	–	0.232	0.157	0.224	13.67–	13.69–	13.73–	13.72–
	–	0.032	0.023	0.035	14.06	14.30	14.15	14.33
083	0.077	0.101	–	–	13.16–	13.36–	–	–
	0.012	0.011	–	–	13.43	13.69		
084	–	–	0.041	0.058	–	–	18.54–	18.60–
	–	–	0.165	0.224			19.18	19.40
085	–	–	0.136	0.194	–	–	16.77–	16.74–
	–	–	0.152	0.235			17.48	17.73
086	0.113	0.135	–	–	12.64–	12.80–	–	–
	0.010	0.013	–	–	12.96	13.18		
087	0.200	0.235	–	–	13.94–	14.29–	–	–
	0.023	0.025	–	–	14.52	15.01		
088	–	–	0.038	0.057	–	–	19.27–	19.32–
	–	–	0.149	0.216			19.85	20.15
089	0.093	0.102	–	–	13.15–	13.61–	–	–
	0.028	0.037	–	–	13.55	14.10		
	0.034	0.040	–	–				
090	–	–	0.128	0.182	–	–	17.00–	16.99–
	–	–	0.156	0.220			17.79	18.01
091	0.141	–	–	–	13.90–	14.33–	–	–
	0.071	–	–	–	14.55	14.92		
092	–	–	0.023	0.033	–	–	17.20–	17.29–

Table 2: **Semi-amplitudes and magnitude ranges**

No.	Semi-amplitudes				Magnitude ranges			
	aV	ag	zr	zg	aV	ag	zr	zg
	–	–	0.159	0.231			17.65	17.89
093	–	–	0.110	0.151	–	–	16.93–	16.86–
	–	–	0.156	0.222			17.57	17.80
094	0.151	0.177	0.116	0.165	12.83–	13.14–	12.65–	13.13–
	0.014	0.020	0.010	0.020	13.23	13.61	12.95	13.55
095	–	–	0.112	0.169	–	–	17.20–	17.11–
	–	–	0.159	0.226			17.87	18.11
096	0.062	0.075	–	–	11.60–	11.76–	–	–
	0.015	0.015	–	–	11.81	12.00		
097	0.196	0.235	–	–	14.41–	14.48–	–	–
	0.050	0.063	–	–	15.18	15.40		
098	–	–	0.065	0.097	–	–	18.76–	18.70–
	–	–	0.152	0.234			19.35	19.62
099	0.073	0.070	0.060	0.088	14.7–	15.2–	14.47–	15.37–
	<0.027	0.027	0.023	0.028	15.2	15.7	14.72	15.72
	0.038	0.024	0.020	0.034				
100	0.082	0.099	–	–	12.17–	12.38–	–	–
	0.023	0.028	–	–	12.52	12.83		
	0.038	0.043	–	–				
101	–	–	0.045	0.062	–	–	19.2–	19.5–
	–	–	0.143	0.217			19.7	20.4
102	0.063	0.065	–	–	14.95–	15.10–	–	–
	0.056	0.062	–	–	15.37	15.60		
103	0.127	0.152	0.104	0.141	13.51–	13.60–	13.60–	13.67–
	0.039	0.051	0.028	0.048	14.00	14.16	13.98	14.12
104	–	–	0.075	0.108	–	–	17.23–	17.58–
	–	–	0.081	0.110			17.69	18.25
105	0.105	0.128	0.108	0.174	13.75–	14.05–	13.73–	14.41–
	0.011	0.014	0.012	0.018	14.08	14.50	14.05	14.87
	0.010	0.007	0.007	0.010				
106	0.039:	0.041:	0.077	0.128	14.6:–	14.65:–	15.17–	15.67–
	0.011:	0.006:	0.010	0.013	14.75:	14.85:	15.41	16.03
107	0.083	0.093	0.050	0.083	13.75–	13.92–	13.73–	13.96–
	0.018	0.019	0.013	0.019	14.05	14.24	13.91	14.20
108	0.088	0.110	–	–	15.10–	15.15–	–	–
	0.087	0.115	–	–	15.65	15.80		
109	–	–	0.081	0.104	–	–	17.18–	17.54–
	–	–	0.062	0.091			17.61	18.12
110	–	–	0.180	0.259	–	–	16.06–	16.84–
	–	–	0.018	0.024			16.53	17.52

Table 3: **Color indices and Galactic latitude**

No.	$J-K$, 2MASS	$B-V$, APASS	$g'-r'$, APASS	$g-V$, ASAS-SN	$g-r$, ZTF	b, deg
010	0.47	0.91	0.72	0.45	0.82	–2.9
051	0.24:	0.48	0.50	–	0.46	–9.1
052	0.46:	–	–	–	0.47	–6.0
053	0.53	–	–	–	0.69	–5.9
054	0.29	0.46	0.25	0.23:	0.29	–9.1
055	0.69	0.76	1.12	–	1.19	+2.1
056	0.35	0.75	0.53	0.30	0.55	–5.1
057	0.55	–	–	–	0.31	–8.4
058	0.47:	0.42	0.27	–	0.27	–12.0
059	0.90	–	–	–	1.60	+1.6
060	0.59	–	–	–	0.69	–7.5
061	0.40	0.59	0.57	0.45	0.62	–4.0
062	0.17	0.39	0.08	0.17	0.11	–15.2
063	0.33	–	–	–	0.60	–6.0
064	0.42	–	–	–	1.02	+5.9
065	0.63	–	–	–	0.37	–10.2
066	–	–	–	–	0.39	+9.1
067	0.53	1.09	–	0.46	0.77	+2.6
068	0.73	–	–	–	1.41	+5.0
069	0.58	0.51	0.57	–	0.90	+1.7
070	0.65	–	–	–	1.04	+4.5
071	0.97	–	–	–	1.30	+5.0
072	0.37	–	–	–	0.98	+3.8
073	0.38	0.68	0.58	–	0.63	+10.7
074	0.91	–	–	–	1.99	+0.9
075	0.36	0.72	0.58	0.36	0.45	–12.5
076	0.45	0.93	0.76	0.37	0.86	+4.0
077	0.69	–	–	–	0.93	+1.1
078	0.71	–	–	–	0.90	+4.1
079	0.43:	–	–	–	0.78	+5.0
080	0.16:	0.41	0.20	–	0.19	+18.1
081	0.39	0.61	0.44	0.33	0.51	+7.7
082	0.18	0.27	0.10	0.15	0.11	+27.5
083	0.20:	0.42	0.28	0.23	–	–5.9
084	–	–	–	–	0.13	+74.4
085	0.74	–	–	–	0.14	+48.5
086	0.21	0.44	0.24	0.21	–	+15.0
087	0.45	0.89	0.78	0.44	–	+7.4
088	–	–	–	–	0.18	+45.2
089	0.60	1.06	1.02	0.49	–	–4.8
090	–	–	–	–	0.14	+34.5
091	0.29	0.61	0.40	0.34	–	+11.2
092	–	0.03	0.54	–	0.16	+44.8
093	–	–	–	–	0.10	+37.6
094	0.39	0.72	0.74	0.35	0.57	+18.7

Table 3: **Color indices and Galactic latitude**

No.	$J-K$, 2MASS	$B-V$, APASS	$g'-r'$, APASS	$g-V$, ASAS-SN	$g-r$, ZTF	b, deg
095	1.25:	–	–	–	0.11	+39.8
096	0.22	0.60	0.27	0.17	–	–0.5
097	0.17	0.40	0.20	0.18	–	–15.9
098	–	–	–	–	0.12	+27.6
099	1.23	0.97	0.91	0.45	0.94	+0.9
100	0.23	0.35	0.18	0.27	–	+14.5
101	–	–	–	–	0.53	+10.8
102	0.23	0.45	0.17	0.20	–	–14.1
103	0.15	0.33	0.04	0.16	0.12	–16.4
104	0.84	–	–	–	0.51	–4.0
105	0.41	0.96	0.71	0.40	0.76	–2.7
106	0.44	0.80	0.50	0.09:	0.58	–3.7
107	0.21	0.44	0.28	0.20	0.24	–24.1
108	0.39	0.21	0.09	0.10	–	–37.0
109	–	–	0.30	–	0.43	–8.1
110	0.49	–	–	–	0.91	+2.2

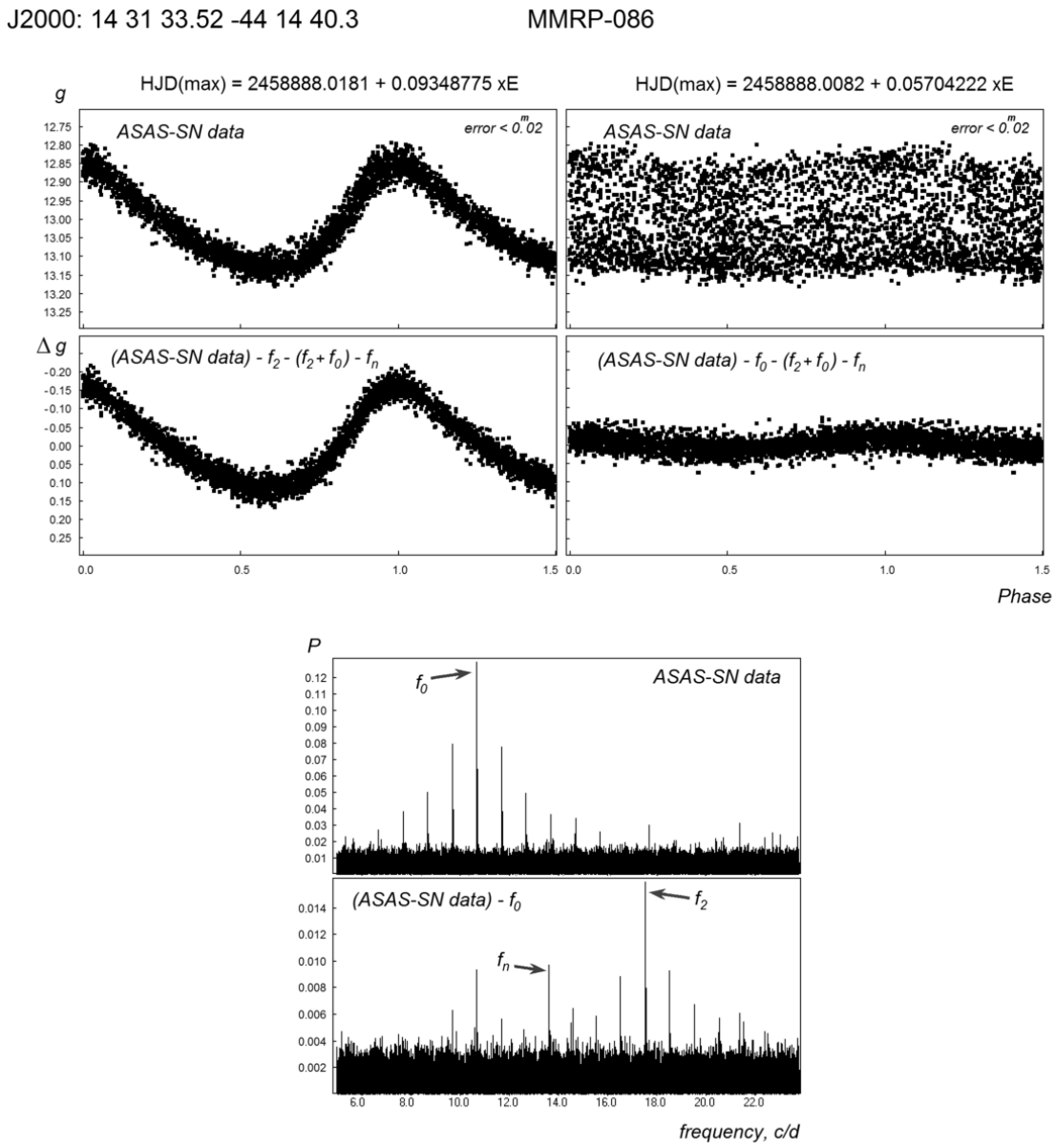

Figure 2. The light curves and power spectra of MMRP-086 (D02n: type) from g-band ASAS-SN data.

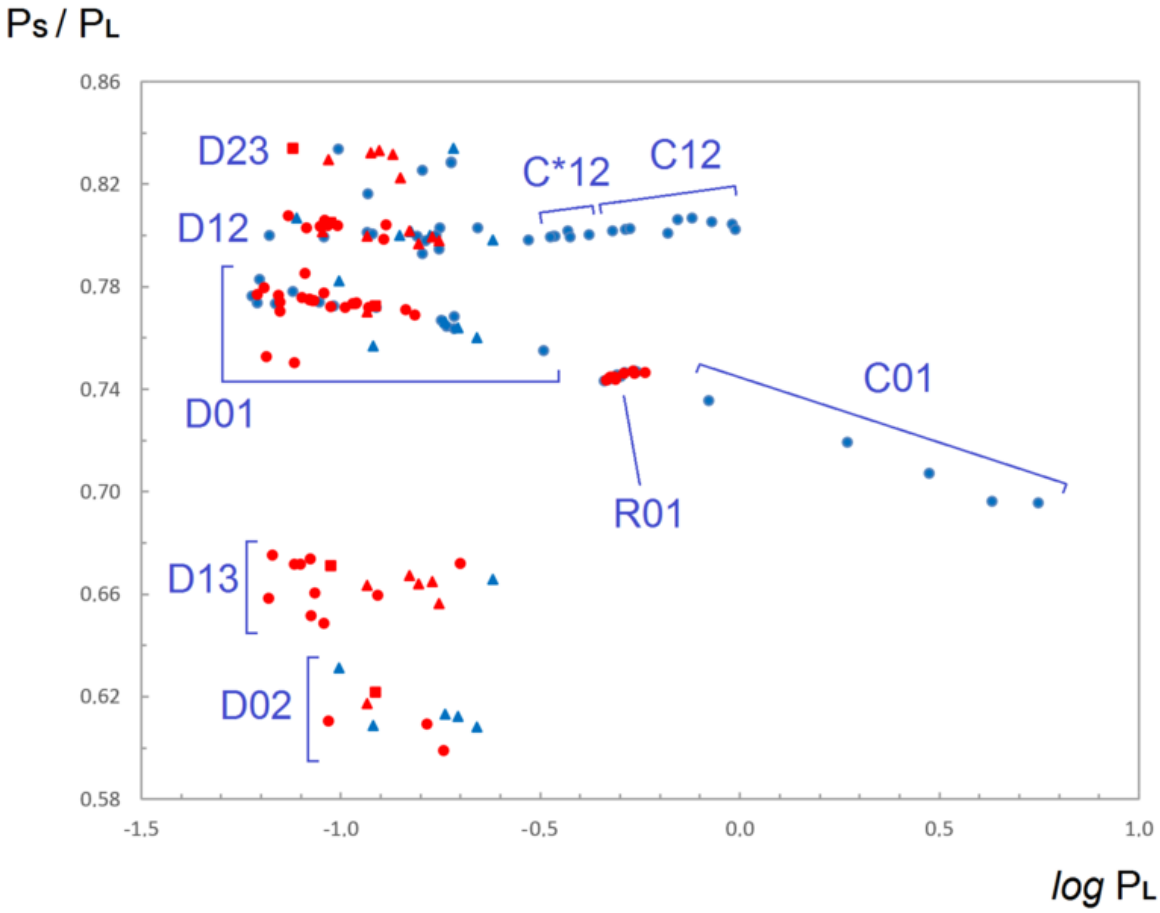

Figure 3. The Petersen diagram for the multi-periodic stars of the MMRP catalog: blue – stars of the MMRP–I catalog, red – stars of the MMRP–II catalog (this paper); circles – double-mode stars, triangles – triple-mode stars, squares – quadruple-mode variables.